

# **Glycerol valorisation: development of selective protocols for acetals production through tailor-made macroreticular acid resins.**

*Assunta Marrocchi,<sup>a</sup> Valeria Trombettoni,<sup>a</sup> Filippo Campana,<sup>a</sup> Valerio Passagrilli,<sup>a</sup> Alireza Nazari,<sup>a</sup> Maria Paola Bracciale,<sup>b</sup> Maria Laura Santarelli,<sup>b</sup> Luigi Vaccaro<sup>a\*</sup>*

<sup>a</sup> Laboratory of Green S.O.C. – Dipartimento di Chimica, Biologia e Biotecnologie, Università degli Studi di Perugia, Via Elce di Sotto 8, 06123 – Perugia – Italy

<sup>b</sup> Dipartimento di Ingegneria Chimica Materiali Ambiente, Università di Roma Sapienza, via Eudossiana 18, 00185 Roma, Italy.

\*Corresponding Author:

Luigi Vaccaro – Laboratory of Green S.O.C. – Dipartimento di Chimica, Biologia e Biotecnologie, Università degli Studi di Perugia, Via Elce di Sotto 8, 06123 – Perugia – Italy;

E-mail: [luigi.vaccaro@unipg.it](mailto:luigi.vaccaro@unipg.it); Web: [greensoc.chm.unipg.it](http://greensoc.chm.unipg.it).

## **Abstract**

Bio-based glycerol and aldehydes have been valorised by acetalization reaction over novel macroporous sulfonated polystyrene-type resins (MR-SP20-SO<sub>3</sub>H and MR-SP50-SO<sub>3</sub>H). The influence of reactants molar ratio, catalyst amount, temperature, and reaction time on the activity and selectivity to acetals have been investigated. Results showed that MR-SP20-SO<sub>3</sub>H and MR-SP50-SO<sub>3</sub>H confirm a high performance in the acetalization of the glycerol derivatives 1,2- propandiol, 1,3-propandiol, 3-methoxy-1,2-propandiol and monoacetin; these catalytic systems enable recover and reuse.

## **Keywords**

*glycerol valorization; furfural; acetalization; heterogeneous catalysis; biomass transformation*

## 1. Introduction

The policies and regulatory requirements that are in force worldwide on the use of renewable energy, are ever more stringent. For example, the European Renewable Energy Directive set rules for EU to achieve a renewable target of 32% by 2030. In this context, biodiesel fuel has attracted considerable attention as a biodegradable, clean burning, low toxic alternative fuel for diesel engines, which can be blended with fossil-based diesel conventional fuels.[1] Driven by these characteristics, the global biodiesel market has a reasonable growth pace. Though the biofuels industry has been strongly impacted by the Covid-19 pandemic, with an 11.6% drop in 2020 from 2019's record production (162 billion L, 41 billion L of which were biodiesel), the output has started to recover robustly in 2021. The fuel demand recovery and stronger market policies are anticipated to boost biofuel rebound by a further 4% in 2022, with a forecast of 45 billion L biodiesel production.[2]

Biodiesel is a mixture of long-chain C10–C22 fatty acid methyl esters (FAMEs). Typically, biodiesel is industrially produced by base-catalyzed transesterification reaction of triglycerides from vegetable oils, animal fats or waste oils with an alcohol (i.e. methanol, ethanol).[3] Crude glycerol (Figure 1) is the byproduct of the reaction, and represents ~10 wt % of the transesterification products. The biodiesel global production has therefore generated a large excess of glycerol, which inevitably affects the sustainability of biodiesel manufacturing. [4-5]

Thus, the scientific community has directed great efforts towards the development of strategies [6-12] to convert glycerol into high added-value products such as fine chemicals, diols, polymer precursors, solvents, fuel additives, and flavouring agents. This is also driven by the favourable toxicological and eco-toxicological profile of glycerol, and by the current need for a transition towards a circular (bio)economy, where waste valorisation plays a pivotal role.[13]

According to various authors, [9,14-25] crude glycerol might represent a suitable, abundant, and low-priced feedstock for biomass acetalization.

Broadly speaking, acetalization denotes the nucleophilic addition of an alcohol or an ortho-ester to a carbonyl compound, in the presence of an acid catalyst, to afford acetals (or ketals) and water byproduct. [26-27] The catalytic acetalization of glycerol, as a tri-alcohol, with an aldehyde or a ketone typically generates a mixture of different cyclic acetals (ketals), consisting of six- or five-membered rings. Such compounds are valuable chemicals that can be used e.g. as fuel additives, “green” solvents, flavouring agents, plasticizers, or as building blocks for surfactants. [9,14-25]

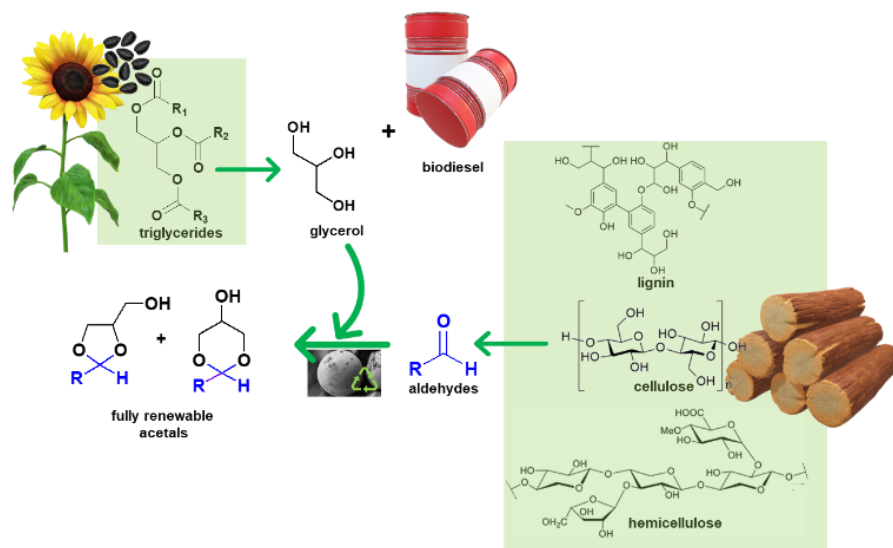


**Figure 1.** Scheme of this work.

However, the synthesis of acetals (ketals) via traditional techniques is not considered a clean and efficient procedure, since the presence of water byproduct can suppress the yield due to the thermodynamic limitations, lead to side transesterification reactions, [7] and hamper the efficiency of the catalyst employed, specifically under heterogeneous catalytic conditions.

In this study, the attention has been focused on the development of sustainable protocols for the use of glycerol **1a** in the acetalization of a set of aldehydes derivable from lignocellulosic biomass. Specifically, we explored furan-based aldehydes **2a-2c** (i.e., furfural, 5-methyl furfural and 5-hydroxymethyl furfural), which can be obtained from the polysaccharide fraction of the lignocellulose, [28] along with aromatic aldehydes such as benzaldehyde (**5a**), p-anisaldehyde (**5b**), vanillin (**5c**), and trans-cinnamaldehyde (**5d**). These latter can be considered as model compounds from lignin depolymerization. [29] (Chart 1).

We also explored the use of the glycerol-derivatives 1,2- propandiol (**1b**), 1,3-propandiol (**1c**), 3-methoxy-1,2-propandiol (**1d**) and monoacetin (**1e**) as alcohols (Chart 1). The rationale behind the substrates' choice is to realize fully renewable acetals (Chart 1), with mutual valorization of glycerol and lignocellulosic biomass.

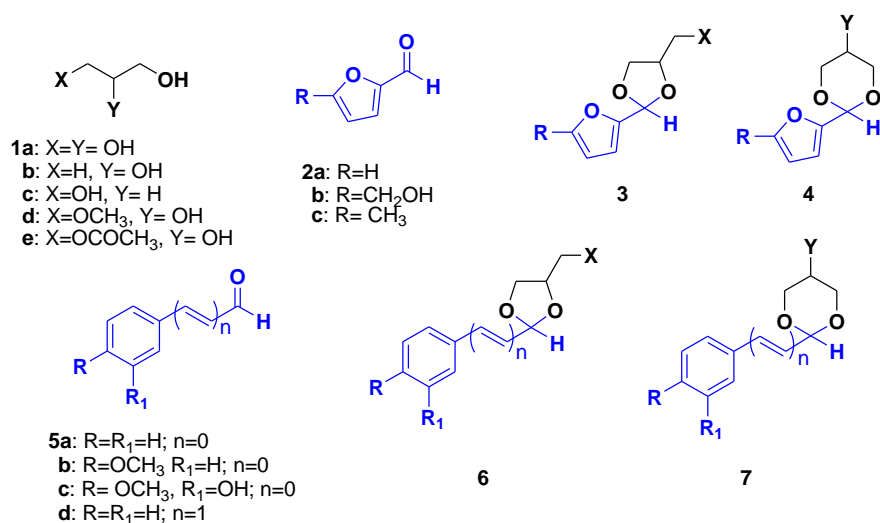


**Chart 1.** Acetals and their precursors.

Concerning the acidic catalyst, we focused on specifically designed heterogeneous systems based on sulfonic acid groups (-SO<sub>3</sub>H catalytic sites) immobilized on polystyrene-type (i.e. Merrifield's type) [30] macroreticular resins. These resins comprise a polymer network obtained by employing a large and rigid 1,4-bis(4-vinylphenoxy)benzene cross-linker which replaces the 1,4-divinyl benzene used in traditional Merrifield's counterparts. The catalytic systems are a new introduction in the family of polystyrene-type resins (namely SPACeR) developed by us and have already proven to be efficient in biomass valorization processes, owing to the ability of the cross-linker to impart the resin a high compatibility with the highly oxygenated bio-based substrates. [31-37]

## 2. Materials and Methods

All reagents were purchased from commercial sources and used without further purification, unless otherwise noted. Commercial Amberlyst-15<sup>®</sup> (4.7 mmol SO<sub>3</sub>H/g, particle size < 0.3 mm) and commercial Dowex 50W-8X (4.4 mmol SO<sub>3</sub>H/g, particle size < 0.25 mm) were purchased at Sigma-Aldrich Co. Elemental microanalyses were performed using Elemental UNICUBE analyzer using atropine, 2,5-bis-2-(5-tertbutylbenzoxazol-yl)-thiophene (BBOT), and phenanthrene as a reference standard, with an accuracy of ca. 2 μmol g<sup>-1</sup>. GLC analyses were performed by using Hewlett-Packard HP 5890A instrument equipped with a capillary column DB-35MS (30 m, 0.53 mm), an FID detector and hydrogen as gas carrier. GLC-EIMS analyses were carried out by using a Hewlett-Packard HP 6890 N Network GC system/5975 Mass Selective Detector equipped with an electron impact ionizer at 70 eV. High resolution scanning

electron microscopy (HR-SEM) images were taken with a field-emission scanning electron microscope (Auriga, Zeiss) operated at 8 kV.

Specific surface area, total pore volume and average pore size were measured by nitrogen adsorption/desorption isotherms at  $-196\text{ }^{\circ}\text{C}$  using a  $\text{N}_2$  adsorption Micromeritics Triflex analyzer (Micromeritics Instrument Corp); data were acquired in the  $p/p_0$  range from 0.01 to 0.99. Isotherm analyses were performed using the 3Flex Version 4.05 software. Samples were previously outgassed at  $200\text{ }^{\circ}\text{C}$  for 4 h

. Fourier-transform infrared (FTIR) analyses were carried out with a Bruker Vertex 70 spectrometer (Bruker Optik GmbH) equipped with a single reflection Diamond ATR cell. Thermogravimetric (TG) analyses were performed using an SDT Q600 (TA Instruments) analyzer.

## **2.1. Catalysts' preparation**

### **2.1.1. Synthesis of macroreticular resin MR-SP.**

A solution of polyvinyl alcohol (PVA,  $M_w = 31.000\text{--}50.000$ ; 1.5 g, 1.5 wt %) and NaCl (4.5 g, 4.5 wt%) in distilled water (100 mL) was introduced in a three-neck flat bottom cylinder-shaped glass vessel. Next, the mixture was heated at  $40\text{ }^{\circ}\text{C}$  under mechanical stirring and  $\text{N}_2$  flux. A pre-mixed solution of styrene (2.4 g, 22.9 mmol or 1 g, 9.6 mmol) and azobisisobutyronitrile (AIBN, 0.1 g; 0.62 mmol, 4.4 wt%) in toluene (1 mL) was then added under stirring and the resulting mixture was kept at  $65\text{ }^{\circ}\text{C}$  for 1 h. After that, a pre-heated ( $65\text{ }^{\circ}\text{C}$ ) solution of 1,4-bis(4-vinylphenoxy) benzene (1.8 g, 5.73 mmol or 3 g, 9.6 mmol) in 9 mL of toluene-cyclohexanol (1:1 v/v) was introduced into the vessel under stirring. The reaction system was kept under mechanical stirring at  $65\text{ }^{\circ}\text{C}$  for 24 h. After the reaction completion, the resin beads were filtered under vacuum, and then washed with water (6 h), THF (6 h) and hexane (6 h) by using a Soxhlet apparatus. Finally, the polymer was dried by a vacuum pump.

### **2.1.2. Synthesis of $-\text{SO}_3\text{H}$ functionalized MR-SP resins.**

The previously synthesized polystyrene resin (0.5 g) was dried over-night at  $50\text{ }^{\circ}\text{C}$ . Then, a swelling agent was added ( $\text{CH}_2\text{Cl}_2$ , 2 mL), and the system was kept under stirring for 1 h at  $60\text{ }^{\circ}\text{C}$ . After the  $\text{CH}_2\text{Cl}_2$  removal, 2.5 mL of 37%  $\text{H}_2\text{SO}_4$  ( $0.09\text{ mmol g}^{-1}$  of polymer) were added dropwise at  $0\text{ }^{\circ}\text{C}$ , and the system was subsequently heated and kept at  $60\text{ }^{\circ}\text{C}$  for 24 h. After the reaction time, the mixture was cooled to r.t., and the obtained MR-SP- $\text{SO}_3\text{H}$  was filtered, washed with water (10 h) using a Soxhlet apparatus, and dried overnight under vacuum at  $80\text{ }^{\circ}\text{C}$ . The degree of

functionalization for MR-SP20-SO<sub>3</sub>H and MR-SP50-SO<sub>3</sub>H catalysts was determined by elemental analysis. The ionic exchange capacity (IEC) was calculated by titration method (see Table S2 in ESI).

### 2.1.3. Representative experimental procedure for the acetalization of aldehydes **2** and **5** with alcohols **1**

The catalytic experiments were performed in vials equipped with a polytetrafluoroethylene (PTFE)-coated magnetic stirring bar. In a typical procedure, 1 or 5 mmol of alcohol **1a-d**, catalyst (5 mol % or 15 mol%), 1 mmol of aldehyde, and 50 wt % of molecular sieves (4Å) were added to the reactor. The reactor was kept in a thermo-statically controlled oil bath heated at either T=50 °C or 100 °C. The reaction mixture was kept under inert atmosphere. After the reaction time completion, the mixture was cooled down to room temperature, the catalyst was filtered, and washed with 4 mL of ethyl acetate. The reaction was monitored by GLC-EIMS analysis.

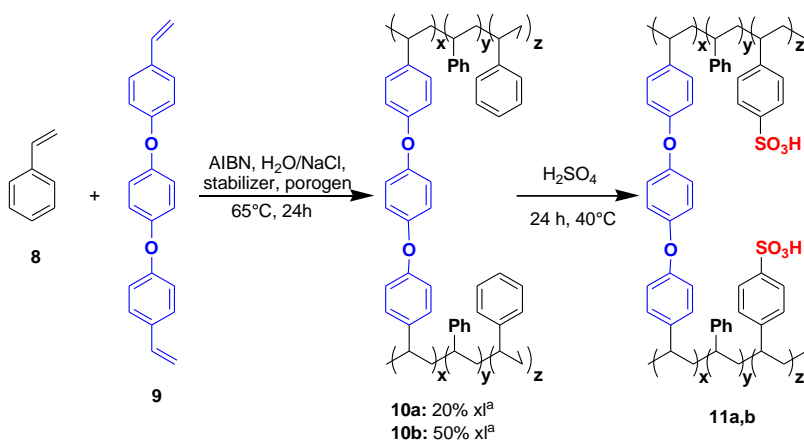
## 3. Results and discussion

In the following section, we report the synthetic procedure as well as the chemical-physical and morphological properties of the novel macroreticular resins prepared with different degrees of cross-linkers (20% and 50%). Next, the catalytic activity of both systems is illustrated in terms of catalyst amount, reactants' molar ratio, reaction temperature and time, and compared with benchmark commercial acidic resins. The section is continued by discussing about the correlations between the catalyst structure and its efficiency.

### 3.1. Synthesis and characterization of sulfonated macroreticular resin catalysts (**11 a,b**)

Scheme 1 depicts the general route followed for the synthesis of the acidic macroreticular heterogeneous catalysts **11a-11b**. First, MR-SP20 (**10a**) and MR-SP50 (**10b**) resins were prepared by free radical copolymerization between styrene (**8**) and 1,4-bis(4-vinylphenoxy) benzene (**9**, 20mol% or 50 mol%) in the presence of azo-bis-isobutyronitrile (AIBN, 4 wt%) as initiator, and using cyclohexanol/toluene mixture (1:1 volume ratio) as porogen system. As a result of SEM connecting to the morphological characteristics and bead size of **10a** and **10b**, polyvinyl alcohol (PVA) acted as the optimal stabilizer in the synthesis of aforementioned copolymers (Table S1). It is noteworthy to mention here that, during the polymerization reaction, the aggregation of polymer microgel colloids (through primarily intramolecular crosslinking reactions) is responsible for the permanent porosity characteristics for a macroreticular resin; several studies have widely demonstrated that microgels formation is strongly dependent on the chemical affinity between the polymeric phase and the porogen.[38] Therefore, to increase swelling of styrene-based polymers in a porogenic solvents and 'solvent porosity' within the resin, toluene was selected as porogen. Moreover, it is known

that cyclohexanol ensures a good phase separation, which is expected to aid the formation of a pore structure with the morphology of a typical macroreticular resin.[39] A spherical form of the polymer beads was achieved by addition of the cross-linker in a single shot, after one hour from the beginning of the styrene polymerization (Table S1, entries 2 and 4) [40]. In addition, good internal and external morphology of the polymer beads were achieved (Table S1, entries 2 and 4).



**Scheme 1.** General synthetic approach to catalysts **11a** and **11b**. <sup>a</sup>Cross-linking.

Further support was given by two bands at  $\sim 1150$  and  $\sim 1200$   $\text{cm}^{-1}$ , which were assigned to the asymmetric and symmetric S=O stretching of sulfonic groups, respectively. The spectrum of bare resin **10a** (Figure S1) is reported for reference. Thermogravimetric analysis (Figure S2) indicated that **11a** and **11b** have good thermal stability up to  $\sim 175^\circ\text{C}$  and  $\sim 200^\circ\text{C}$ , respectively, i.e. the temperatures at which begins the loss of sulfonic groups.

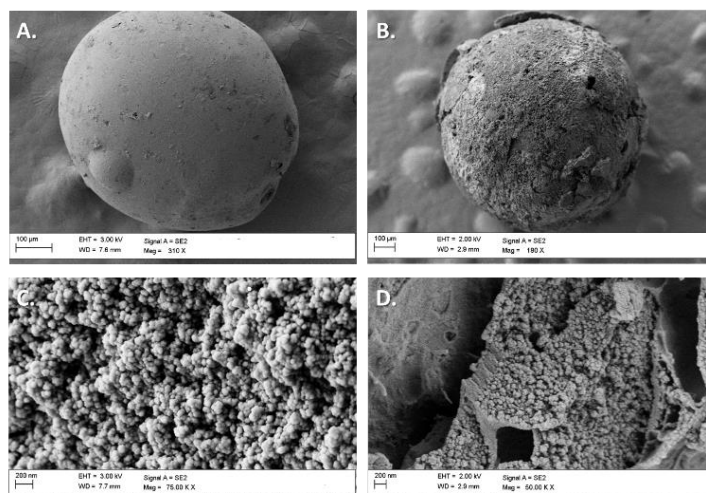


**Figure 2.** Representative SEM images of external and internal morphologies of MR-SP20-SO<sub>3</sub>H (A, C) and MR-SP50-SO<sub>3</sub>H (B, D).

### 3.2. Acetalization of furan-containing aldehydes (2a-c)

**Catalyst screening.** The activity of the novel catalytic systems (**11a** and **11b**) was tested in the reaction between glycerol (**1a**) and furfural (**2a**) to give (2-(furan-2-yl)-1,3-dioxolan-4-yl)methanol (**3a**, Figure 3), an important added value acetal having specific chemical-physical properties which make it suitable as fuel additive. [19, 22, 41]

At this stage, it is worthy to highlight that, based on previous findings, [34] the reaction was performed in the presence of molecular sieves (4Å) and under inert gas (N<sub>2</sub>) to trap produced water from the system, and, hence, enhancing the process efficiency. The screening was carried out under solvent-free conditions, by employing fivefold excess glycerol and 5 mol% amount of catalysts at 100 °C (Table S3, Figure 3). Under these conditions, catalyst MR-SP20-SO<sub>3</sub>H (**11a**) has proved to be very efficient, providing furfural conversion into products up to ~90% in a short time (4h). (Table S3, entry 1).

Under the same conditions, MR-SP50-SO<sub>3</sub>H (**11b**) demonstrated a lower efficiency, enabling a maximum 70% conversion of **2a** into products (Table S3, entry 2). The decrease in conversion might stem from, at least in part, the higher degree of cross-linking of **10b** compared to **10a**, that confers the resin a higher rigidity, ultimately leading to a poorer reactants' accessibility to the catalytic sites.



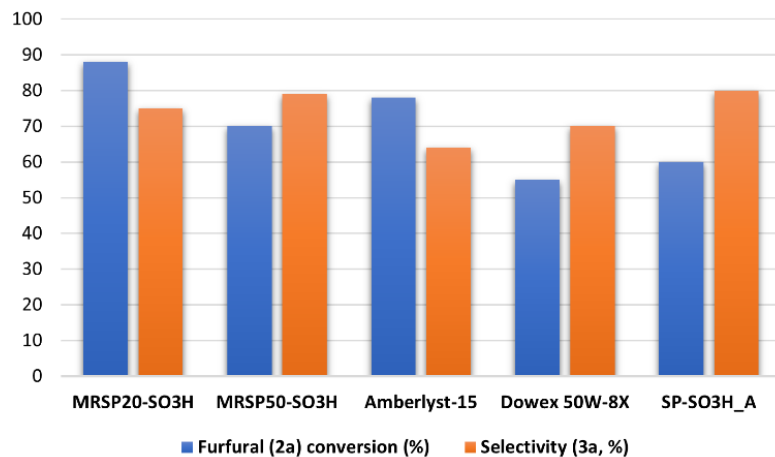
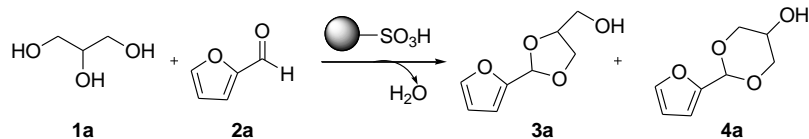


**Figure 3.** Catalyst screening for the acetalization of furfural (**2a**) with glycerol (**1a**). Reaction conditions: **1a:2a**=5:1, 5 mol% catalyst, 100°C, 4h. Data obtained by GLC and GLC-EIMS analyses.

More importantly, the reaction was also performed using commercially available macroreticular Amberlyst-15 and gel-type Dowex 5WX8 as benchmark polystyrene-based catalytic systems. In addition, the activity of **11a** and **11b** was compared with that of SP-SO<sub>3</sub>H\_A, i.e., a gel-type catalyst previously developed by our group, which possesses the same cross-linker of **11a** and **11b**, namely 1,4-bis(4-vinylphenoxy) benzene [34] (Table S3, entries 3-5).

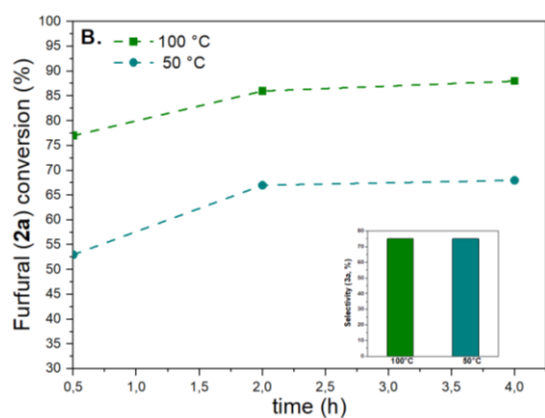
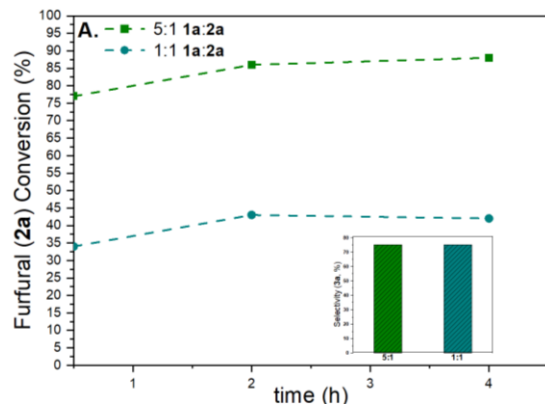
As a result of comparison, macroreticular catalysts enabled better results in terms of **2a** conversion towards the products compared to gel-type resins. However, the selectivity achieved was similar (Table S3, entries 1-3 vs 4 and 5, respectively).

Interestingly, Amberlyst-15 gave a lower **2a** conversion (78% vs 88%, Table S3) and a poorer selectivity towards **3a** (64% vs 75%) compared to MR-SP50-SO<sub>3</sub>H **11a**. Since Amberlyst-15 used in this study has also a cross-linking degree of ~20% (see Experimental section), the enhanced efficiency may be ascribed to the presence of 1,4-bis(4-vinylphenoxy) benzene cross-linker in **11a**. On the other hand, by comparing the results of using the two gel-type resins it was demonstrated that SP-SO<sub>3</sub>H\_A assured a better catalytic efficiency (60% conversion of **2a**, 80% selectivity towards **3a**). This might be attributed, at least to some extent, to the different type of resins' cross-linking.

In fact, Dowex 50W-8X features 1,4-divinylbenzene (DVB) as cross-linker, which is less polar and smaller than the 1,4-bis(4-vinylphenoxy) benzene in SP-SO<sub>3</sub>H\_A, likely leading to a hindered access of reactants to the catalyst sites. To certify catalytic activity of the systems, almost negligible **2a** conversion was observed in the absence of catalyst (Table S3, entry 6).

On these bases, MR-SP20-SO<sub>3</sub>H (**11a**) was chosen for the optimization study of this reaction. Catalytic efficiency was evaluated by varying key parameters such as **1a**:**2a** molar ratio, catalyst amount, temperature, and reaction time. The most significant data are presented in Table S4.

As it is possible to observe in Figure 4A, the use of a fivefold excess of **1a** rather than equimolar amount of **1a** and **2a** allows a higher conversion of **2a** (88% vs 42%, Table S4, entries 4 and 8). On the other hand, no variation in the selectivity towards **3a** (75%) was noted (Figure 4A, inset).



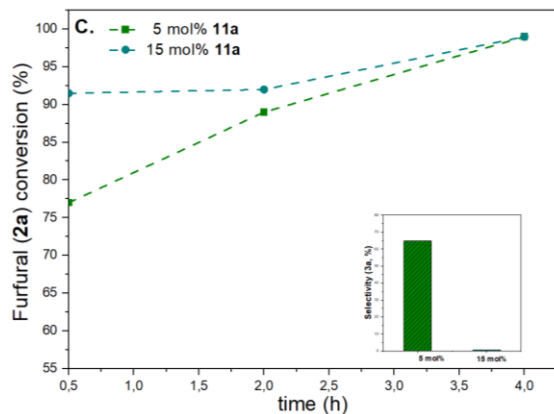


**Figure 4.** Influence of experimental conditions on the MRSP20SO<sub>3</sub>H activity for the acetalization of **2a** with **1a**. (A) Effect of the mole ratio on conversion of **2a** into **3a** and **4a** and on selectivity towards **3a**. Reaction conditions: 5 mol% catalyst, 100 °C; (B.) Effect of temperature on conversion of **2a** into **3a** and **4a** and on selectivity towards **3a**. Reaction conditions: **1a:2a**= 5:1, 5 mol% catalyst. (C.) Effect of catalyst amount on conversion of **2a** into **3a** and **4a** (plot c1) and on selectivity towards **3a** (plot c2). Reaction conditions: **1a:2a**= 5:1, 100 °C.

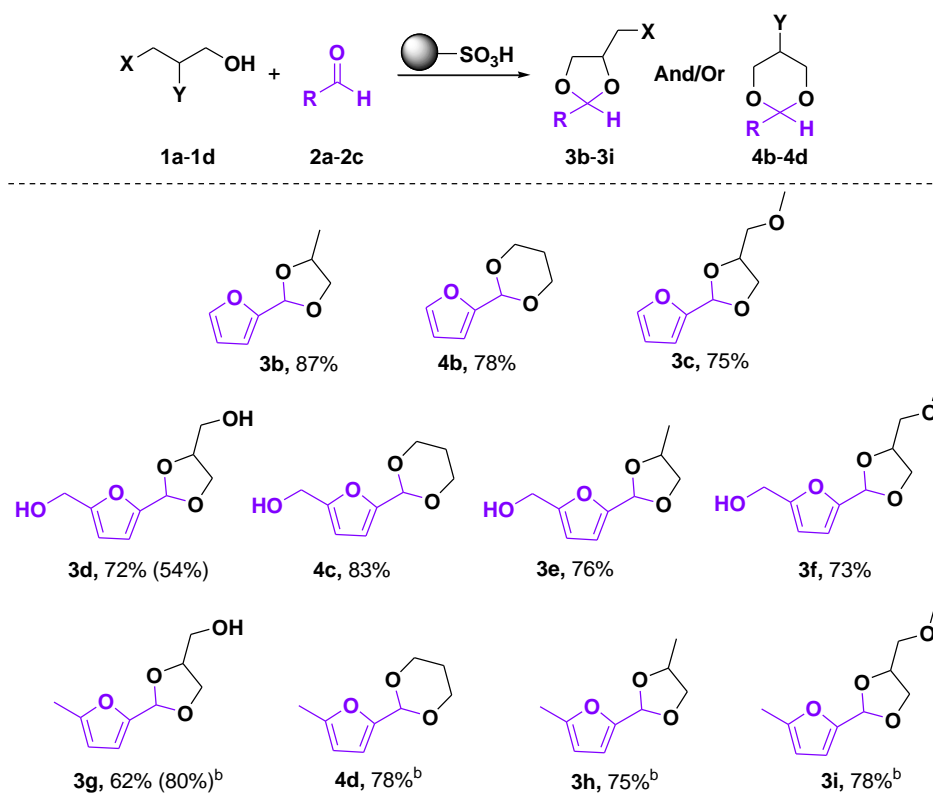
On the other hand, by lowering the reaction temperature from 100 °C to 50 °C (Figure 4B), the catalyst has proved to be less efficient, enabling a maximum conversion of 68% (Table S4, entry 2), though no relevant effect in the selectivity towards **3a** was observed (Figure 4B, inset). When the catalyst amount was increased from 5 mol% to 15 mol%, furfural **2a** rapidly converted into a dark insoluble solid, and no acetalization product was observed. Indeed, the combination of more acidic conditions and relatively high temperatures, caused the degradation of **2a** (Figure 4C and Table S4, entry 5).

The optimal result in terms of both conversion and selectivity, therefore, was achieved by using 5:1 **1a** to furfural molar ratio and 5 mol% of **11a** catalyst at 100 °C. There was negligible internal mass transfer effect associated with this process. In fact, under the optimal reaction conditions, the activity of the catalyst in its original bead shape was essentially the same as the powder form, which was obtained by grinding the beads on a mortar.

**Substrate scope.** To broaden the scope of catalyst **11a**, the optimized reaction protocol was extended to other substrates. For the aldehydes, we used 5-hydroxymethyl furfural (**2b**) and 5-methylfurfural (**2c**). For the alcohols, besides glycerol **1a**, we considered 1,2-propanediol, (**1b**) 1,3-propanediol (**1c**) and 3-methoxy-1,2-propanediol (**1d**). The corresponding acetals **3b-i** [18, 23] and **4b-d** are reported in Scheme 3.

Scheme 2 shows that the catalyst **11a** confirmed a high efficiency in the reaction of furfural **2a** with the three diols **1b-1d**, enabling good conversion values into products **3b-3c** and **4d** (75-87%). The reaction of 5-hydroxymethyl

furfural (**2b**) with **1a-1d** also gave satisfactory results, enabling the efficient formation of acetals **3d**, **3e**, **3f** and **4c** (72-83%). However, poor selectivity towards the five-membered ring acetal was observed with glycerol **1a** (54%). (Scheme 2). The use of 5-methylfurfural (**2c**) required a further tuning of the reaction conditions, and optimal results were obtained by decreasing the reaction temperature to 50°C and employing an equimolar amount of reactants. Under these conditions, **11a** enabled aldehyde conversion values in the range 62%-78%, with a selectivity of 80% towards the five-membered acetal when using glycerol (Scheme 2).



**Scheme 2.** Synthesis of furan-based acetals (**3b-i**, **4b-d**) using catalyst **11a**. <sup>a</sup>Conversion data obtained by GLC analyses. Selectivity in parenthesis. Reaction conditions: 5 eq. of **1a-c**, 5 mol% catalyst, 100°C, 4h. <sup>b</sup> Reaction conditions: 1 eq. of **1a-c**, 5 mol% catalyst, 50 °C, 4h.

**Catalyst recycling.** Applying the optimal conditions for acetalization of **2a** and glycerol (Table S4, entry 4), the recycling of catalyst **11a** was studied. After the first run, the catalyst was separated from the reaction mixture by filtration, washed with ethyl acetate, dried overnight under vacuum, and reused. The catalysts substantially retained its efficiency after three representative consecutive runs (Table 1).

**Table 1.** Recycling of MR-SP20-SO<sub>3</sub>H.<sup>a</sup>

Entry	Run	C (%) <sup>b</sup>	S(%) <sup>b</sup>
1	I	88	75:25
2	II	88	74:26
3	III	86	74:26

<sup>a</sup> Reaction conditions: 5 eq. of **1a**, 5 mol% catalyst, 100°C, 4h. <sup>b</sup> Data obtained by GLC analyses.

### 3.3. Acetalization of benzaldehyde (**5a**) and derivatives (**5b-d**).

**Catalyst screening.** Based on the satisfactory results obtained for the acetalization of furan-based aldehydes, we explored the acetalization benzaldehyde (**5a**) with glycerol (**1a**), targeting (2-phenyl-1,3-dioxolan-4-yl)methanol (**6a**), typically used as fragrance, and having chemical-physical characteristics which may enable its use as solvent (Figure 5).[42]

A major challenge in this transformation [43] is to achieve good selectivity towards acetals **6a** or **7a**. In fact, benzaldehyde easily undergoes oxidation in the presence of acidic water. Therefore, the combined use of molecular sieves and nitrogen flow was of crucial importance to scavenge produced water in the reaction. By performing the reaction in the presence of **11a** (5 mol%) and using a 5:1 **1a**:**5a** molar ratio, under solvent-free conditions, a benzaldehyde conversion of 94% and a selectivity towards **6a** of 80% was achieved after 4h. (Table S5, entry 1). Under the same conditions, catalyst MR-SP-50SO<sub>3</sub>H (**11b**) showed a comparable efficiency, enabling a benzaldehyde conversion of 90% and a selectivity towards **6a** of 78% (Table S5, entry 2). No traces of benzoic acid were detected in both cases. The study of the effect of the change of the mole ratio of **1a** to **5a** on the reaction outcome enabled the identification of an interesting trend. In fact, it was found that by employing an equimolar amount of **1a** and **5a**, both the **5a** conversion (84%) and selectivity towards **6a** (72%) decreased over **11a** (Table S5, entry 1). Moreover, the formation of a small percentage of benzoic acid was observed (4%). On the other hand, **11b** enabled a selectivity of

84% towards **6a**, and a total selectivity towards acetals was maintained, though a slight decrease in **5a** conversion (85%) was observed (Table S5, entry 2). For comparison purposes, the reaction was also carried out using Amberlyst-15. In this case, poorer conversions were obtained by using both 5:1 **1a:5a** and 1:1 **1a:5a** molar ratio (85% and 67%, respectively), though the selectivity towards **6a** remained comparable (~80%). Notably, when using an equimolar amount of reactants, Amberlyst-15 behaved similarly to **11a**, leading to the formation of benzoic acid (7%). (Table S5, entry 3). Reference gel-type catalysts Dowex 5WX8 and SP-SO<sub>3</sub>H\_A also gave less satisfactory results (Table S5, entries 4 and 5).

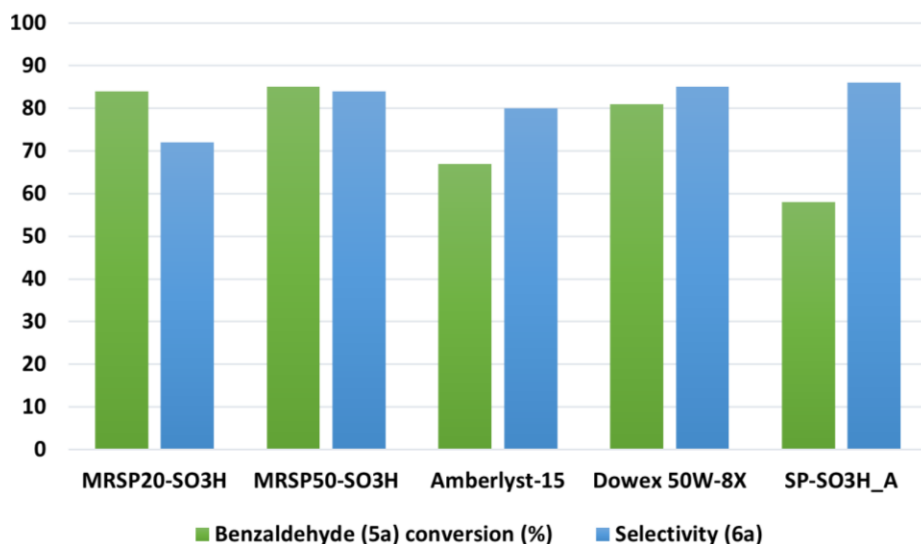
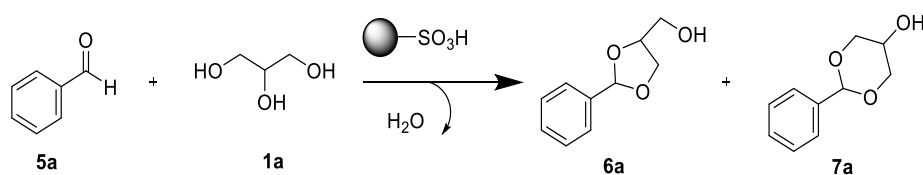


**Figure 5.** Catalyst screening for the acetalization of benzaldehyde (**5a**) with glycerol (**1a**). Reaction conditions: **1a:5a**=1:1, 5 mol% catalyst, 100°C, 4h. Data obtained by GLC and GLC-EIMS analyses.

Therefore, **11b** was chosen for the continuation of this study. The advantage of using **11b** is that the use of excess glycerol is avoided.

The MR-SP-50SO<sub>3</sub>H catalytic efficiency was further studied by varying key parameters such as catalyst amount, temperature, and reaction time. The most significant data are presented in Table S6.

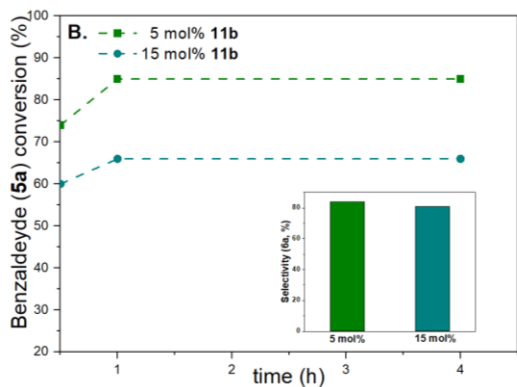
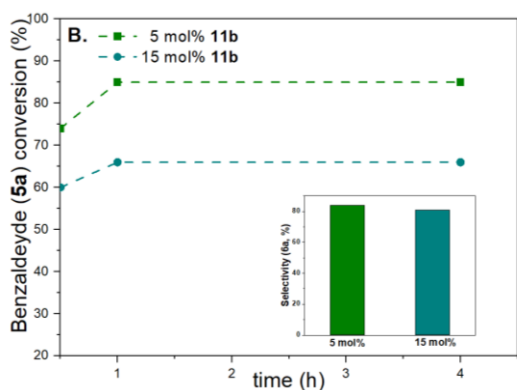
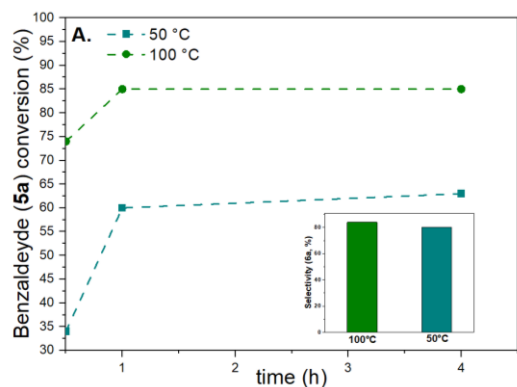


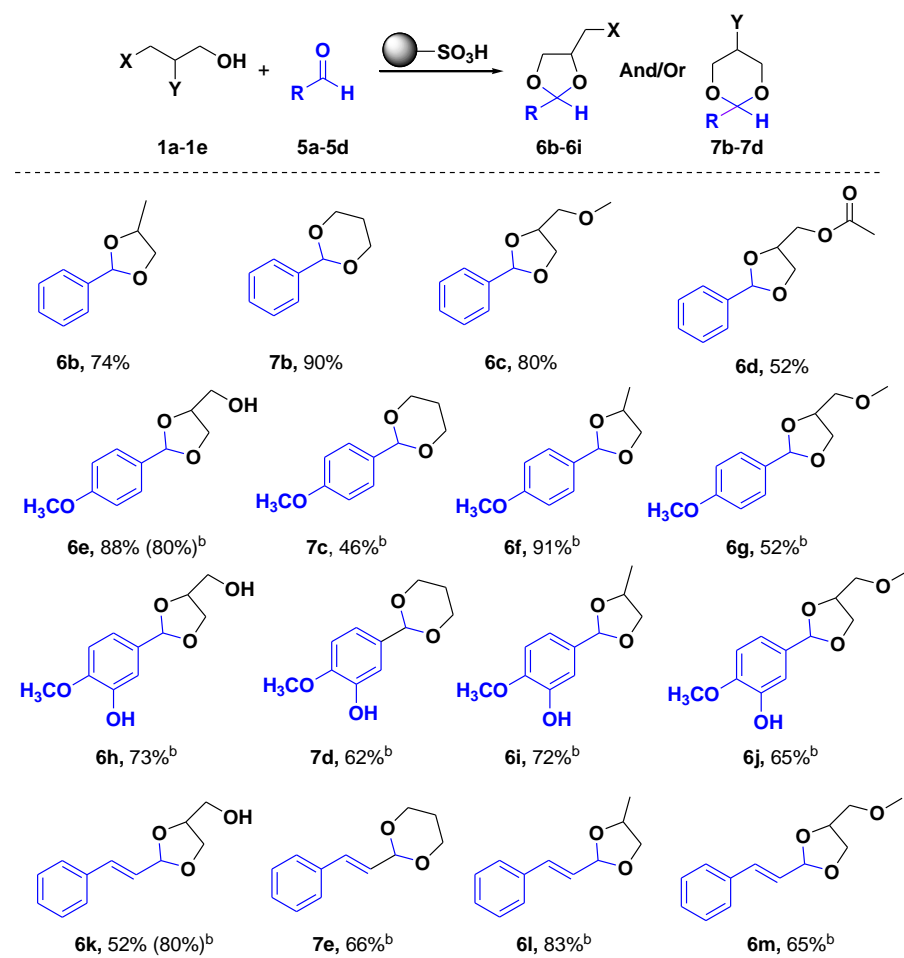
**Figure 6.** Influence of the experimental conditions on MRSP50SO<sub>3</sub>H activity in the acetalization of **5a**. A.) Effect of temperature on conversion of **5a** into **6a** and **7a** and on selectivity towards **6a**. Reaction conditions: **5a**:**1a**= 1:1 molar ratio, 5 mol% catalyst. B.) Effect of catalyst amount on conversion of **5a** into **6a** and **7a** and on selectivity towards **6a**. Reaction conditions: **5a**:**1a**= 1:1 molar ratio, 100°C.

For example, the decrease of the reaction temperature from 100°C to 50 °C (Figure 6A) gave a lower conversion value (34%, 1h and 63% 4h; Table S6, entry 5). On the other hand, a comparable selectivity towards **6a** was observed after

4h (Figure 6A, inset). Using 15%mol of **11b**, a lower **5a** conversion was observed (66%) (Figure 6B, plot b1; Table S6, entry 8). Selectivity towards **6a** is closely comparable (Figure 6B, inset). Interestingly, by employing a 1:1 **1a:5a** molar ratio, reaction time exerted a clear influence on selectivity towards **6a**, with maximum values achieved at shorter reaction times (Table S6, entries 5-8).

Consequently, the prime results in terms of both **5a** conversion (85%) and selectivity towards **6a** (94%) was reached by using 1:1 **1a** to benzaldehyde molar ratio and 5 mol% of **11b** catalyst at 100 °C, after 1h.

**Substrate scope.** The optimized protocol was also extended to other substrates. For the aldehydes, we used *p*-anisaldehyde (**5b**), vanillin (**5c**), and *trans*-cinnamaldehyde (**5d**). For the alcohols we considered 1,2-propanediol (**1b**), 1,3-propanediol (**1c**), 3-methoxy-1,2-propanediol (**1d**) and 3-acetoxy-1,2-propanediol (**1e**). The corresponding acetals **6** [19, 21, 24] and **7** are reported in Scheme 3.





**Scheme 3.** Acetalization of aromatic aldehydes **5a-5d** with **1a-1e**, over catalyst **11b**. Selectivity in parenthesis. <sup>a</sup>Reaction conditions: 1 eq. of **1a-d**, 5 mol% catalyst, 100°C. <sup>b</sup> Reaction conditions: 5 eq. of **1a-d**, 15 mol% catalyst, 100°C

Catalyst **11b** confirmed a high efficiency in the reaction of benzaldehyde **5a** with all the diols under investigation, except **1e**, for which a still acceptable 52% was achieved.

The use of *p*-anysaldehyde (**5b**), vanillin (**5c**), and trans-cynnammaldehyde (**5d**) required a further tuning of the reaction conditions, and optimal results were obtained by using a five-fold excess alcohol and increasing the catalyst amount (15 mol%). Under these conditions, **11b** enabled aldehyde conversion values in the range 46%-91%, with selectivities towards the five-membered ring acetals of ~80% when using glycerol.

In all cases, no oxidation by-products were observed.

**Catalyst recycling.** By using the optimal conditions for the reaction between **5a** and glycerol (Table S6, entry 7), the recycling of catalyst **11b** was investigated. After the first run, the catalyst was separated from the reaction mixture by filtration, washed with ethyl acetate, dried overnight under vacuum, and reused. The catalyst substantially retained its efficiency after three representative consecutive runs (Table 2).

**Table 2.** Recycling of MR-SP50-SO<sub>3</sub>H.<sup>a</sup>

Entry	Run	C (%) <sup>b</sup>	S (%) <sup>b</sup>
1	I	85	94:6
2	II	85	94:6
3	III	84	92:8

<sup>a</sup> Reaction conditions: 1:1 **1a:5a**, 5 mol% catalyst, 100 °C, 1 h. <sup>b</sup>Data obtained by GLC analyses.

#### 4. Conclusions

We have introduced a novel class of highly-spaced macroreticular sulphonated resins (MR-SP20-SO<sub>3</sub>H and MR-SP50-SO<sub>3</sub>H) as heterogeneous catalysts. The new acidic resins feature the 1,4-bis(4-vinylphenoxy)benzene cross-

linker, which is larger and more polar than the 1,4-divinyl benzene cross-linker typically used for classic Merrifield resins. Their catalytic activity was investigated in the acetalization reaction of bio-based aldehydes with glycerol and its derivatives, aiming at the mutual valorisation of glycerol and lignocellulosic biomass, in the frame of a circular bio-economy approach. Generally, they have proven to be efficient and versatile catalyst systems for a broad range of substrates.

### **Conflicts of interest.**

There are no conflicts of interest to declare under Conflicts of interest.

### **ACKNOWLEDGMENTS**

The Università degli Studi di Perugia and MIUR are acknowledged for financial support to the project AMIS, through the program “Dipartimenti di Eccellenza - 2018-2022”. A.N.K. and L.V. acknowledge fundings from the European Union's Horizon 2020 Research and Innovation programme under the Marie Skłodowska-Curie entitled STiBNite (N\_ 956923).

### **Appendix A. Supplementary data**

The following is Supplementary data to this article: Table S1: Data for the synthesis of copolymers MR-SP20 (**10a**) and MR-SP50 (**10b**) and their chemical-physical and morphological characteristics; Table S2: Microanalytical data, acid capacity, and textural properties of **11a,b**; Figure S1: FTIR patterns of **11a,b** and bare resins **10a**; Figure S2: TGA plots for **11a,b**; Table S3: Catalyst screening for the reaction between glycerol **1a** and furfural **2a**; Table S4: Catalytic activity of MR-SP20-SO<sub>3</sub>H (**11a**) in the reaction between glycerol (**1a**) and furfural (**2a**). Table S5: Catalyst screening for the reaction between glycerol (**1a**) and benzaldehyde (**5a**). Table S6: Catalytic activity of MR-SP50-SO<sub>3</sub>H (**11b**) in the reaction between glycerol (**1a**) and benzaldehyde (**5a**).

## REFERENCES

- [1] Directive (EU) 2018/2001 of the European Parliament and of the Council of 11 December 2018 on the promotion of the use of energy from renewable sources (accessed December 8, 2021). <https://eur-lex.europa.eu/legal-content/EN/TXT/?uri=CELEX%3A02018L2001-20181221>.
- [2] IEA. Transport biofuels. [https://www.spglobal.com/platts/en/market-insights/latest\\_news/agriculture/070516-world-biodiesel-productionconsumption-to-rise-14-by-2020-oecd-fao](https://www.spglobal.com/platts/en/market-insights/latest_news/agriculture/070516-world-biodiesel-productionconsumption-to-rise-14-by-2020-oecd-fao) (last accessed December 8, 2021)
- [3] D. Singh, D. Sharma, S. L. Soni, S. Sharma, K. P. Sharma, A. A. Jhalani, A review on feedstocks, production processes, and yield for different generations of biodiesel. *Fuel*, 262 (2020) 116553.
- [4] H.W. Tan, A.R. Abdul Aziz, M.K. Aroua, Glycerol production and its applications as a raw material: A review, *Renew. Sustain. Energy Rev.* 27 (2013) 118–127.
- [5] Y. Zheng, X. Chen, Y. Shen, Commodity chemicals derived from glycerol, an important biorefinery feedstock, *Chem. Rev.* 110 (2010) 1807 (Erratum: *Chemical Reviews* (2008) 108 (5253)).
- [6] N.M. Kosamia, M. Samavi, B.K. Uprety, S.K. Rakshit, Valorization of biodiesel byproduct crude glycerol for the production of bioenergy and biochemicals, *Catalysts* 10 (2020) 1–20.
- [7] M.R. Karimi Estahbanati, M. Feilizadeh, F. Attar, M.C. Iliuta, Current developments and future trends in photocatalytic glycerol valorization: photocatalyst development, *Ind. Eng. Chem. Res.* 59 (2020) 22330–22352.
- [8] M. Checa, S. Nogales-Delgado, V. Montes, J.M. Encinar, Recent advances in glycerol catalytic valorization: A review, *Catalysts*. 10 (2020) 1–41.
- [9] I. Fatimah, I. Sahroni, G. Fadillah, M.M. Musawwa, T.M.I. Mahlia, O. Muraza, Glycerol to solketal for fuel additive: Recent progress in heterogeneous catalysts, *Energies*. 12 (2019) 2872.
- [10] S.C. D'Angelo, A. Dall'Ara, C. Mondelli, J. Pérez-Ramírez, S. Papadokonstantakis, Techno-economic analysis of a glycerol biorefinery, *ACS Sustain. Chem. Eng.* 6 (2018) 16563–16572.
- [11] C.H. Zhou, H. Zhao, D.S. Tong, L.M. Wu, W.H. Yu, Recent advances in catalytic conversion of glycerol, *Catal. Rev.* 55 (2013) 369–453.

- [12] F. Sun, H. Chen, Organosolv pretreatment by crude glycerol from oleochemicals industry for enzymatic hydrolysis of wheat straw, *Bioresour. Technol.* 99 (2008) 5474–5479.
- [13] Y. Geng, J. Sarkis, R. Bleischwitz, How to globalize the circular economy, *Nature*. 565 (2019) 5–7.
- [14] Q. Peng, X. Zhao, D. Li, M. Chen, X. Wei, J. Fang, K. Cui, Y. Ma, Z. Hou, Synthesis of bio-additive fuels from glycerol acetalization over a heterogeneous Ta/W mixed addenda heteropolyacid catalyst, *Fuel Process. Technol.* 214 (2021) 106705.
- [15] J. Kaur, A.K. Sarma, M.K. Jha, P. Gera, Valorisation of crude glycerol to value-added products: Perspectives of process technology, economics and environmental issues, *Biotechnol. Reports*. 27 (2020) e00487.
- [16] J. Kowalska-Kuś, A. Held, K. Nowińska, A continuous-flow process for the acetalization of crude glycerol with acetone on zeolite catalysts, *Chem. Eng. J.* 401 (2020) 126143.
- [17] Z. Miao, Z. Li, M. Liang, J. Meng, Y. Zhao, L. Xu, J. Mu, J. Zhou, S. Zhuo, W. Si, Ordered mesoporous titanium phosphate material: A highly efficient, robust and reusable solid acid catalyst for acetalization of glycerol, *Chem. Eng. J.* 381 (2020) 122594.
- [18] H. Song, F. Jin, Q. Liu, H. Liu, Zeolite-catalyzed acetalization reaction of furfural with alcohol under solvent-free conditions, *Mol. Catal.* 513 (2021) 111752.
- [19] C.A. Akinawo, L. Mosia, O.A. Alimi, C.O. Oseghale, D.P. Fapojuwo, N. Bingwa, R. Meijboom, Eco-friendly synthesis of valuable fuel bio-additives from glycerol, *Catal. Commun.* 152 (2021) 106287.
- [20] A. Ghosh, A. Singha, A. Auroux, A. Das, D. Sen, B. Chowdhury, A green approach for the preparation of a surfactant embedded sulfonated carbon catalyst towards glycerol acetalization reactions, *Catal. Sci. Technol.* 10 (2020) 4827–4844.
- [21] B. Wang, S. Ma, Q. Li, H. Zhang, J. Liu, R. Wang, Z. Chen, X. Xu, S. Wang, N. Lu, Y. Liu, S. Yan, J. Zhu, Facile synthesis of “digestible”, rigid-and-flexible, bio-based building block for high-performance degradable thermosetting plastics, *Green Chem.* 22 (2020) 1275–1290.

- [22] M.A.R. Jamil, A.S. Touchy, S.S. Poly, M.N. Rashed, S.M.A.H. Siddiki, T. Toyao, Z. Maeno, K. Ichi Shimizu, High-silica HB zeolite catalyzed methanolysis of triglycerides to form fatty acid methyl esters (FAMES), *Fuel Process. Technol.* 197 (2020) 106204.
- [23] K.S. Arias, A. Garcia-Ortiz, M.J. Climent, A. Corma, S. Iborra, Mutual valorization of 5-hydroxymethylfurfural and glycerol into valuable diol monomers with solid acid catalysts, *ACS Sustain. Chem. Eng.* 6 (2018) 4239–4245.
- [24] Y. Zong, L. Yang, S. Tang, L. Li, W. Wang, B. Yuan, G. Yang, Highly efficient acetalization and ketalization catalyzed by cobaloxime under solvent-free condition, *Catalysts*, 8 (2018), 48.
- [25] B.L. Wegenhart, S. Liu, M. Thom, D. Stanley, M.M. Abu-Omar, Solvent-free methods for making acetals derived from glycerol and furfural and their use as a biodiesel fuel component, *ACS Catal.* 2 (2012) 2524–2530.
- [26] D. M. Clode, Carbohydrate cyclic acetal formation and migration, *Chem. Rev.* 79 (1979) 491–513.
- [27] P.G. Wuts, T.W. Greene, *Greene's protective groups in organic synthesis*, John Wiley & Sons, 2006.
- [28] J.J. Bozell, G.R. Petersen, Technology development for the production of biobased products from biorefinery carbohydrates—the US Department of Energy's "top 10" revisited, *Green Chem.* 12 (2010) 539–55.
- [29] Z. Sun, A. De Santi, S. Elangovan, K. Barta, Bright side of lignin depolymerization : toward new platform chemicals, *Chem. Rev.* 118 (2018) 614–678.
- [30] R. B. Merrifield, Solid phase peptide synthesis. I. The synthesis of a tetrapeptide, *J. Am. Chem. Soc.* 85 (1963) 2149-2154.
- [31] F. Valentini, F. Ferlin, E. Tomarelli, H. Mahmoudi, M. Bagherzadeh, M. Calamante, L. Vaccaro, A waste-minimized approach to Cassar-Heck reaction based on POLITAG-Pd(0) heterogeneous catalyst and recoverable acetonitrile azeotrope, *ChemSusChem.* 14 (2021) 3359–3366.
- [32] H. Mahmoudi, F. Valentini, F. Ferlin, L.A. Bivona, I. Anastasiou, L. Fusaro, C. Aprile, A. Marrocchi, L. Vaccaro, A tailored polymeric cationic tag-anionic Pd(II) complex as a catalyst for the low-leaching Heck-Mizoroki coupling in flow and in biomass-derived GVL, *Green Chem.* 21 (2019) 355–360.

- [33] F. Valentini, H. Mahmoudi, L.A. Bivona, O. Piermatti, M. Bagherzadeh, L. Fusaro, C. Aprile, A. Marrocchi, L. Vaccaro, Polymer-supported bis-1,2,4-triazolium ionic tag framework for an efficient Pd(0) catalytic system in biomass derived  $\gamma$ -valerolactone, *ACS Sustain. Chem. Eng.* 7 (2019) 6939–6946.
- [34] V. Trombettoni, D. Sciosci, M.P. Bracciale, F. Campana, M.L. Santarelli, A. Marrocchi, L. Vaccaro, Boosting biomass valorisation. Synergistic design of continuous flow reactors and water-tolerant polystyrene acid catalysts for a non-stop production of esters, *Green Chem.* 20 (2018) 3222–3231.
- [35] A. Marrocchi, P. Adriaensens, E. Bartollini, B. Barkakati, R. Carleer, J. Chen, D.K. Hensley, C. Petrucci, M. Tassi, L. Vaccaro, Novel cross-linked polystyrenes with large space network as tailor-made catalyst supports for sustainable media, *Eur. Polym. J.* 73 (2015) 391–401.
- [36] M. Tassi, E. Bartollini, P. Adriaensens, L. Bianchi, B. Barkakaty, R. Carleer, J. Chen, D.K. Hensley, A. Marrocchi, L. Vaccaro, Synthesis, characterization and catalytic activity of novel large network polystyrene-immobilized organic bases, *RSC Adv.* 5 (2015) 107200–107208.
- [37] M. Alonzi, M.P. Bracciale, A. Broggi, D. Lanari, A. Marrocchi, M.L. Santarelli, L. Vaccaro, Synthesis and characterization of novel polystyrene-supported TBD catalysts and their use in the Michael addition for the synthesis of Warfarin and its analogues, *J. Catal.* 309 (2014) 260–267.
- [38] Sherrington, D.C. Preparation, structure and morphology of polymer supports, *Chem. Commun.*, (1998) 2275–2286
- [39] Q. Liu, L. Wang, A. Xiao, H. Yu, Q. Tan, A hyper-cross-linked polystyrene with nano-pore structure, *Eur. Pol. J.* 44 (2008) 2516–2522.
- [40] P. Šálek, D. Horák, J. Hromádková, Novel preparation of monodisperse poly(styrene-co-divinylbenzene) microspheres by controlled dispersion polymerization, *Polym. Sci.* 60 (2018) 9–15.
- [41] A.L. Maksimov, A.I. Nekhaev, D.N. Ramazanov, Y.A. Arinicheva, A.A. Dzyubenko, S.N. Khadzhiev, Preparation of high octane oxygenate fuel components from plant derived polyols, *Pet. Chem.* 51 (2011) 61–69.
- [42] A.M. Api, D. Belsito, S. Biserta, D. Botelho, M. Bruze, G.A.B. Jr, J. Buschmann, A. Cancellieri, M.L. Dagli, M. Date, W. Dekant, C. Deodhar, A.D. Fryer, S. Gadhia, L. Jones, K. Joshi, M. Kumar, A. Lapczynski, M. Lavelle,

I. Lee, D.C. Liebler, H. Moustakas, M. Na, T.M. Penning, G. Ritacco, J. Romine, N. Sadekar, T.W. Schultz, D. Selechnik, F. Siddiqi, I.G. Sipes, G. Sullivan, Y. Thakkar, Y. Tokura, F.W. Ave, N. York, RIFM fragrance ingredient safety assessment , benzaldehyde glyceryl acetal , CAS Registry Number 1319-88-6, 153 Food Chem. Toxicol. 153 (2021) 112173.

[43]J. Deutsch, A. Martin, H. Lieske, Investigations on heterogeneously catalysed condensations of glycerol to cyclic acetals, J. Catal. 245 (2007) 428–435.